NO LOAD BEHAVIOR PREDICTION OF LARGE FIVE-LEGGED TRANSFORMERS USING TOPOLOGICAL TRANSIENT MODELS

Sergey Zirka, Dennis Albert+, Alexander Fröhlich*

Dnipro National University, Department of Physics and Technology
Nauky av. 72, 49050 Dnipro, Ukraine, e-mail: zirka@email.dp.ua

+OMICRON electronics GmbH
Oberes Ried 1, 6833 Klaus, Austria, e-mail: dennis.albert@omicronenergy.com

*Graz University of Technology, Institute of Electrical Power Systems,
Inffeldgasse 18, 8010 Graz, Austria, e-mail: a.froehlich@tugraz.at

***Abstract* - The work proposes a method of reproducing the no-load losses and currents of large five-legged transformers with the use of their transient models. This aim is achieved by employing topological transformer models based on a dynamic hysteresis model (DHM) and taking into account equivalent transformer capacitances. It is proposed to reproduce initially the measured total losses by using DHM means, and then to determine an equivalent per phase capacitance value that provides a best possible coincidence of calculated and measured current waveforms.**

I. INTRODUCTION

The choice of the core representation is an initial crucial stage in development of transient model of any transformer. As a minimum, the model should replicate, if not predict, no-load losses and currents, which is especially important for large five-legged units.

Most of the time-stepping finite element solvers are too slow and do not reproduce the so-called excess losses, which are the main loss component in high permeability grain-oriented (HGO) steels employed in large transformers. An efficient alternative is to build transformer transient models on the base of a Dynamic Hysteresis Model (DHM) included in 2019 in ATP/ATPDraw program [1] as L(i) Zirka-Moroz nonlinear branch. Its peculiarities are outlined in Section II-A.

When modeling 300 MVA and 786 MVA transformers studied in this work, significant capacitive components were observed in their no-load currents. Therefore, to replicate the measured line (terminal) currents, it is necessary to supplement transformer models with equivalent (per-phase) capacitances. Since their value C is a single fitting parameter, it is easily estimated starting with the value found in the FAT.

Before starting the modeling as a whole, it is critically important to select the proper steel from the DHM menu. It was found that only HGO steels should be used in the models of the large transformers under consideration, whereas using conventional GO steels fails in obtaining acceptable currents.

II. STRUCTURE AND DETAILS OF THE MODELS

A. The composite DHM implemented into ATP/ATPDraw

According to the loss and field separation principle, the total magnetic field (H) formed by the DHM is the sum of the following three components [2]:

$$H = H_{\rm h}(B) + K_{\rm loss}\left[\frac{d^2}{12\rho}\frac{dB}{dt} + \delta\cdot g(B)\left|\frac{dB}{dt}\right|^{0.5}\right] \qquad (1)$$

The field $H_{\rm h}(B)$ is created by the history-dependent static hysteresis model. At high flux densities $B(t)$, dependence $H_{\rm h}(B)$ is extended by a single-valued saturation curve. The terms in brackets represent classical eddy-current and excess fields as detailed in [2]. Multiplier $K_{\rm loss}$ is the loss coefficient, which allows the user to fit the DHM and thus the whole transformer model to the measured losses.

It was supposed that HGO steel 27ZDKH85 was used in both transformers considered. Specific losses W of this steel are shown in Fig. 1. The no-load losses P_0 measured for 300 MVA and 786 MVA transformers are indicated by isolated dots in the inset of Fig. 1. The lines in the inset are P_0 values evaluated with the transformer model outlined in Section II-B using $K_{\rm loss}$ = 0.926 and 0.85 respectively.

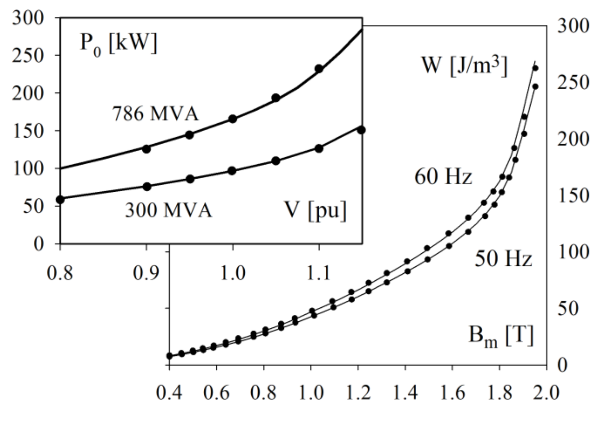

Fig.1. Specific losses W of the steel and no-load transformer losses P_0

The concave loss curves in the inset reflect the voltage and frequency dependence of the DHM (1) illustrated in Fig. 1.

B. DHM-based transformer models

A topological ATPDraw model of the step-up 786 MVA unit (Yd11) with inner (22.8 kV) delta winding and outer (525 kV) wye-connected winding is shown in Fig. 2.

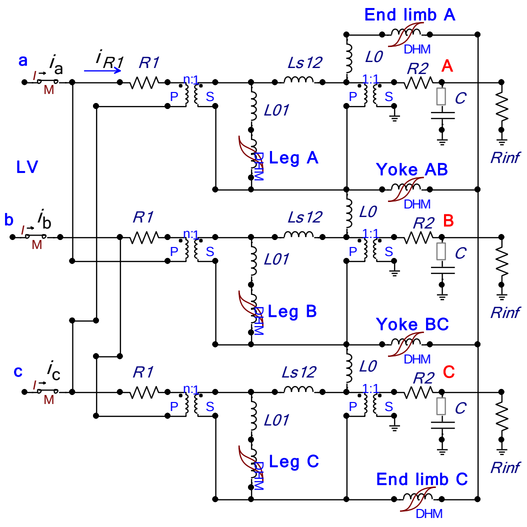

Fig. 2. ATPDraw model of 786 MVA, Yd11 transformer

All major elements of the model are explained in [3]. A similar model of the three-winding 300 MVA transformer can be found in [4].

C. The effect of transformer capacitances

Additional elements of the model are equivalent per-phase capacitances *C*. They are placed at high-voltage (HV) terminals A, B, and C because of the largest capacitive contribution brought by the HV bushings [5], [6]. The introduction of capacitances is necessitated by the fact that at C = 0 the waveforms of the calculated line currents are quite different from the measured currents (Fig. 3 shows currents in lines A and B only because of the limited space).

However, with added capacitances (C = 1900 pF is easily found by trials and errors) the line currents at no-load become quite close to the measured ones (refer Fig. 4).

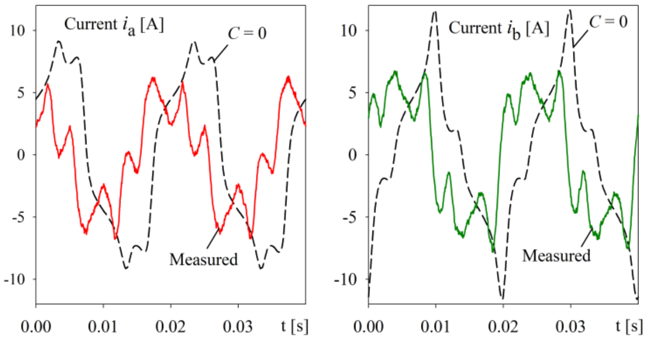

Fig. 3. Measured and calculated no-load line currents at C =0

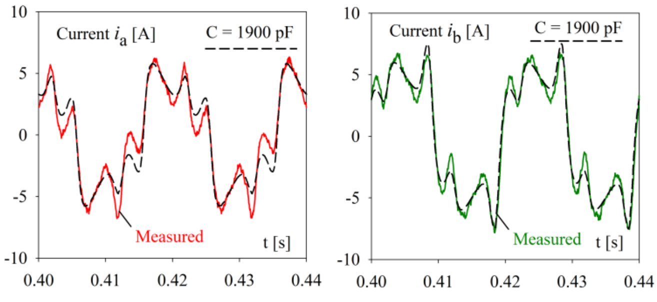

Fig. 4. Measured and calculated no-load line currents at C = 1900 pF

Practically the same results are obtained if 0.27 mm thick steel H1 Carlite is used in the model with K_{loss} = 0.69. However, conventional GO steel M5 (35Z145), for which K_{loss} should be decreased to 0.35, is not suitable for the model because of the large line currents.

A single period of the calculated line current $i_a(t)$ in Fig. 4 (left) is also shown by the dashed curve 1 in Fig. 5 (left). For comparison, the current in the A-phase winding resistor R1 (curve 2) and the referred magnetizing current in the DHM of leg A (curve 3) are also shown in Fig. 5 (left).

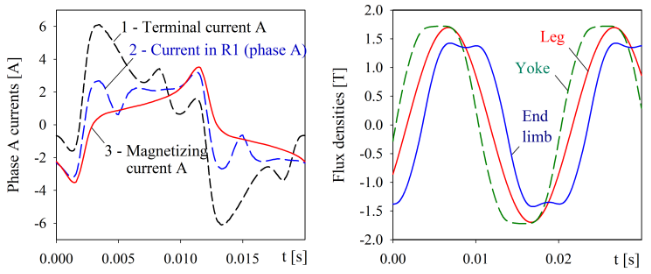

Fig. 5. Phase currents (left) and flux densities (right) of the 5-legged unit

As can be seen in Fig. 5, there is nothing common between the regular magnetizing current (curve 3) and the currents shown by curves 1 and 2 (the latter waveform is typical for the five-legged transformer with inner wye-connected winding as that in the 300 MVA unit modeled). Because of the interphase interaction in the model of Fig. 2 and due to the masking effect of the excited delta-winding, it is difficult, if not impossible, to recognize the magnetizing current using the measured line currents.

In addition to the typical per-phase power pattern (P_a<P_b<P_c), the model with capacitances has shown a similar pattern observed for the terminal rms currents (I_a<I_b<I_c).

Fig. 5 (right) depicts flux densities in the leg A, yoke AB, and the left end limb. The latter two are non-sinusoidal and have different maxima, necessitating the use of the voltage-dependent DHM.

Additional transformer modeling carried out at elevated voltages has revealed experimental uncertainties caused, most probably, by imperfect core demagnetization. So, the model proposed seems to be the first to replicate the currents and losses in a wide range of experimental conditions.

REFERENCES

[1] H. K. Høidalen, L. Prikler, and F. Peñaloza, *ATPDRAW Version 7.0 for Windows. Users' Manual*, NTNU, 2021, Trondheim, Norway.

[2] S. E. Zirka, Y. I. Moroz, N. Chiesa, R. G. Harrison, and H. K. Høidalen, "Implementation of inverse hysteresis model into EMTP – Part II: Dynamic model," *IEEE Trans. Power Del.*, vol. 30, no. 5, pp. 2233-2241, 2015.

[3] S. E. Zirka, D. Albert, Y. I. Moroz, and H. Renner, "Further improvements in topological transformer model covering core saturation," *IEEE Access*, vol. 10, pp. 64018-64027, 2022.

[4] S. E. Zirka, Y. I. Moroz, J. Elovaara, M. Lahtinen, R. A. Walling, H. Høidalen, D. Bonmann, C. M. Arturi, and N. Chiesa, "Simplified models of three-phase, five-limb transformer for studying GIC effects", Int. J. Electric Power and Energy Systems, vol. 103, pp. 168-175, 2018.

[5] C. Carrander, Magnetizing currents in power transformers – Measurements, simulations, and diagnostic methods, Doctoral Thesis, Stockholm, Sweden 2017.

[6] G. Rovišan, G. Plišić, F. Kelemen, "Influence of capacitive no-load current component in large power transformers," Procedia Engineering 202, pp. 176–182, 2017.